Optics Communications 428 (2018) 131–135

Contents lists available at ScienceDirect

Optics Communications

journal homepage: www.elsevier.com/locate/optcom

Reconfigurable microwave photonic mixer based on dual-polarization dual-parallel Mach–Zehnder modulator

Zhan Shi, Sha Zhu, Ming Li, Ning Hua Zhu, Wei Li *

State Key Laboratory on Integrated Optoelectronics, Institute of Semiconductors, Chinese Academy of Sciences, Beijing 100083, China
The School of Electronic, Electrical and Communication Engineering, University of Chinese Academy of Sciences, Beijing 100049, China

ARTICLE INFO

Keywords:
Microwave photonics
DP-DPMZM
Mixer
Balanced mixer
I/Q mixer
Image reject

ABSTRACT

We report a reconfigurable microwave photonic mixer with multiple functions and wide bandwidth. By changing the photodetection configuration, the mixer can be conveniently reconfigured to realize four functions: single-ended mixing, I/Q mixing, double balanced mixing and image rejection mixing. Furthermore, the filter-free system has a wide bandwidth and the ability to perform both frequency up-conversion and down-conversion. The proposed reconfigurable mixer is based on a dual-polarization dual-parallel Mach–Zehnder modulator (DP-DPMZM). The optical signal is modulated by the DP-DPMZM and split into two orthogonally polarized signals, which are combined by a 90° optical hybrid and detected by photodetectors. The experimental results show that the mixer has a wide bandwidth from 2 GHz to 30 GHz with a 30 dB spur suppression, and the image rejection ratio of the image rejection mixer is over 30 dB.

1. Introduction

Microwave mixer plays an important role in microwave and millimeter-wave systems such as radar, remote sensing and satellite communication. It is used to perform frequency up-conversion or down-conversion, in which an intermediate frequency (IF) signal is up-converted to the radio frequency (RF) band, or an RF signal down-converted to the IF band. Compared with conventional microwave mixers, microwave photonic (MWP) mixers have the advantage of large operating bandwidth, high isolation, flexibility and reconfigurability, and immunity to electromagnetic interference [1–4].

MWP mixers have been previously demonstrated based on various structures such as cascaded optical modulators [5–7], parallel optical modulators [8], an integrated optical modulator [9–11], etc. The common cascaded structure has the problem of high mixing spurs and high conversion loss. Parallel configuration can overcome these problems. However, in parallel structures, the optical path length difference between two arms is instable, which would influence the performance of the mixer. Besides, the use of two modulators renders the system bulky and complicated. Therefore, WMP mixer based on an integrated modulator is preferable.

Most previous works on microwave photonic mixer only realized single-ended mixing [12–15]. Frequency mixers with more advanced functions, such as in-phase/quadrature (I/Q) mixing, balanced mixing and image rejection mixing, are desired. Specifically, I/Q mixer is useful for I/Q modulation and demodulation, and can be applied in zero IF transmitters [16,17]; balanced mixer can suppress dc components and improve the performance of the mixer [18]; image rejection mixer (often in frequency down conversion) can be used to suppress unwanted image frequency signals [19,20]. A system with all the aforementioned functions would significantly reduce the complexity and cost of a communication system, and is thus desired in practical applications.

Recently, a reconfigurable mixer which can perform single-ended mixing, I/Q mixing, balanced mixing and image rejection mixing was demonstrated [21]. However, this mixer utilizes two modulators in parallel, which renders the system complicated and unstable. In [22], an optimized design implementing an integrated modulator was demonstrated, in which the optical path separation is minimized. However, frequency up-conversion is not possible in this structure. Besides, both mixers implemented tunable optical bandpass filter, which has a limited roll-off factor, and this limited the operating bandwidth of the systems.

In this Letter, we propose a reconfigurable microwave photonic mixer based on a dual-polarization dual-parallel Mach–Zehnder modulator (DP-DPMZM). The mixer has a large operating bandwidth since no electrical or optical filters are applied. Besides, both frequency up-conversion and down-conversion can be realized in this structure by adjusting the bias voltage of the DP-DPMZM. By changing the detection configuration of the output optical signals, the system can be

* Corresponding author at: State Key Laboratory on Integrated Optoelectronics, Institute of Semiconductors, Chinese Academy of Sciences, Beijing 100083, China.
E-mail address: liwei05@semi.ac.cn (W. Li).

https://doi.org/10.1016/j.optcom.2018.07.055
Received 14 May 2018; Received in revised form 16 July 2018; Accepted 17 July 2018
Available online 19 July 2018
0030-4018/

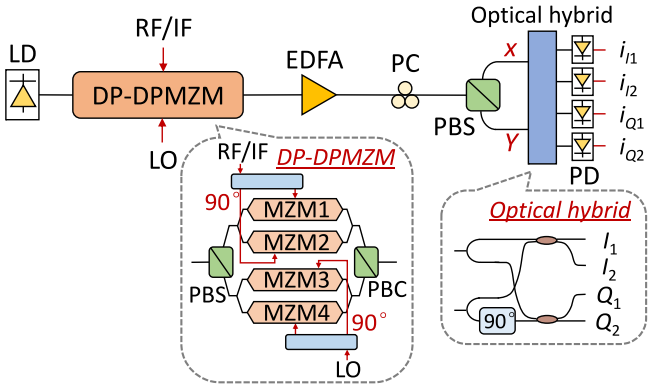

Fig. 1. Schematic diagram of the proposed reconfigurable MWP mixer. LD, laser diode; DP-DPMZM, dual-polarization dual-parallel Mach–Zehnder modulator; EDFA, erbium doped fiber amplifier; PC, polarization controller; PBS, polarization beam splitter; PD, photo detector; PBC, polarization beam combiner; MZM, Mach–Zehnder modulator.

reconfigured between four functions: single-ended mixing, I/Q mixing, double balanced mixing and image rejection mixing. The feasibility of the proposed reconfigurable mixer is theoretically analyzed and experimentally verified.

2. Principle

Fig. 1 shows the schematic configuration of our proposed reconfigurable MWP mixer. The optical carrier (OC) emitted from the laser diode (LD) is split and fed to the two dual-parallel Mach–Zehnder modulators (DPMZMs) of the DP-DPMZM. The two DPMZMs are modulated by RF/IF signal and LO signal, respectively. Two orthogonally polarized carrier-suppressed single sideband (CS-SSB) modulated signals are generated and amplified by an erbium doped fiber amplifier (EDFA). A polarization controller (PC) and a polarization beam splitter (PBS) are used to separate the two orthogonally polarized CS-SSB signals, which are then fed to the two input ports of the 90° optical hybrid. The optical signals from the output ports are recovered by photodetectors (PDs).

The DP-DPMZM consists of a PBS, two DPMZMs, and a polarization beam combiner (PBC). For one DPMZM, an electrical signal is applied to a 90° electrical hybrid and divided into two signals with quadrature phase, which are respectively fed to the two sub Mach–Zehnder modulators (MZMs) of the DPMZM. Both sub MZMs are biased at minimum transmission point. By adjusting the phase difference between the two sub MZMs, a CS-SSB modulation can be realized. For frequency mixing, we apply an RF/IF signal and a LO signal to the upper and lower DPMZM, respectively. The output optical field of the upper DPMZM is thus written as

$$\begin{aligned} E_S &= E_{MZM1} + E_{MZM2}e^{j\varphi_1} \\ &= \frac{\sqrt{2}}{8}E_0(t)\{[e^{j\beta_S\cos\omega_S t} + e^{j(-\beta_S\cos\omega_S t+\pi)}] \\ &\quad + [e^{j\beta_S\sin\omega_S t} + e^{j(-\beta_S\sin\omega_S t+\pi)}]e^{j\varphi_3}\} \\ &= \begin{cases} \frac{\sqrt{2}}{2}E_0J_1(\beta_S)e^{j(\omega_c+\omega_S)t+j\frac{\pi}{2}}, & \varphi_1 = \frac{\pi}{2} \\ \frac{\sqrt{2}}{2}E_0J_1(\beta_S)e^{j(\omega_c-\omega_S)t+j\frac{\pi}{2}}, & \varphi_1 = -\frac{\pi}{2} \end{cases}, \end{aligned} \tag{1}$$

where $E_0(t) = E_0e^{j\omega_c t}$ is the optical carrier with a amplitude of E_0 and an angular frequency of ω_c, V_S and ω_S are the amplitude and angular frequency of the RF/IF signal, $\beta_S = \pi V_S/V_\pi$ is the modulation index of the sub MZMs with a half-wave voltage of V_π, φ_1 is the phase difference between the two sub MZMs of the upper DPMZM, $J_1(\beta_S)$ is the first-order Bessel of the first kind. Here, the small signal modulation condition is assumed. As can be seen, when φ_1 is $\pi/2$ or $-\pi/2$, a CS-SSB signal with only the +1st or −1st sideband left is generated.

Similarly, the optical signal from the lower DPMZM is given by

$$E_L = \begin{cases} \frac{\sqrt{2}}{2}E_0J_1(\beta_L)e^{j(\omega_c+\omega_L)t+j\frac{\pi}{2}}, & \varphi_2 = \frac{\pi}{2} \\ \frac{\sqrt{2}}{2}E_0J_1(\beta_L)e^{j(\omega_c-\omega_L)t+j\frac{\pi}{2}}, & \varphi_2 = -\frac{\pi}{2} \end{cases}, \tag{2}$$

where $\beta_L = \pi V_L/V_\pi$, ω_L and V_L is the angular frequency and amplitude of the LO signal, φ_2 is the phase difference between the two sub MZMs of the lower DPMZM. For simplicity, we assume that only the positive component is generated from the upper DPMZM, and Eq. (1) becomes

$$E_S = \frac{\sqrt{2}}{2}E_0J_1(\beta_S)e^{j(\omega_c+\omega_S)t+j\frac{\pi}{2}}. \tag{3}$$

Since E_S and E_L are orthogonally polarized, the optical field of the DP-DPMZM can be written as

$$E_{DP-DPMZM} = \hat{x}E_S + \hat{y}E_L. \tag{4}$$

A PC is implemented to make sure the x polarization axis of $E_{DP-DPMZM}$ aligns with that of the PBS. In this way, E_S and E_L are separated by the PBS and respectively fed to the two input ports of the 90° optical hybrid. The optical signals from the output ports of the 90° optical hybrid are given by

$$\begin{aligned} E_{I_1} &\propto J_1(\beta_S)e^{j(\omega_c+\omega_S)t+j\frac{\pi}{2}} + J_1(\beta_L)e^{j(\omega_c\pm\omega_L)t+j\frac{\pi}{2}}, \\ E_{I_2} &\propto J_1(\beta_S)e^{j(\omega_c+\omega_S)t+j\frac{\pi}{2}} + J_1(\beta_L)e^{j(\omega_c\pm\omega_L)t-j\frac{\pi}{2}}, \\ E_{Q_1} &\propto J_1(\beta_S)e^{j(\omega_c+\omega_S)t+j\frac{\pi}{2}} + J_1(\beta_L)e^{j(\omega_c\pm\omega_L)t+j\pi}, \\ E_{Q_2} &\propto J_1(\beta_S)e^{j(\omega_c+\omega_S)t+j\frac{\pi}{2}} + J_1(\beta_L)e^{j(\omega_c\pm\omega_L)t}. \end{aligned} \tag{5}$$

If each of the output signals is detected by a PD, the photocurrents can be written as

$$\begin{aligned} i_{I_1} &\propto J_1(\beta_S)J_1(\beta_L)\cos[(\omega_S \pm \omega_L)t], \\ i_{I_2} &\propto -J_1(\beta_S)J_1(\beta_L)\cos[(\omega_S \pm \omega_L)t], \\ i_{Q_1} &\propto J_1(\beta_S)J_1(\beta_L)\sin[(\omega_S \pm \omega_L)t], \\ i_{Q_2} &\propto -J_1(\beta_S)J_1(\beta_L)\sin[\omega_S \pm \omega_L t]. \end{aligned} \tag{6}$$

It can be seen that for each of the four output ports, a single-ended mixer is realized. The phase difference between i_{I_1} and i_{Q_1} is 90°, so an I/Q mixer can be realized. Since the phase difference between i_{I_1} and i_{I_2} is 180°, a balanced mixer can be achieved if a balanced PD is used. Moreover, the system can switch between frequency up-conversion and down-conversion by changing φ_2.

Based on the I/Q mixer, an image rejection mixer for frequency down-conversion can be accomplished by combining i_{I_1} and i_{Q_1} with a 90° electrical hybrid. To demonstrate the feasibility of image rejection mixing, an additional image signal is applied to the upper DPMZM. The output signal of the upper DPMZM becomes

$$E_S' = \frac{\sqrt{2}}{2}E_0J_1(\beta_S)[e^{j(\omega_c+\omega_S)t+j\frac{\pi}{2}} + e^{j(\omega_c+\omega_{IM})t+j\frac{\pi}{2}}], \tag{7}$$

where $\omega_{IM} = 2\omega_L - \omega_S$ is the angular frequency of the image signal. i_{I_1} and i_{Q_1} thus becomes

$$\begin{aligned} i_{I_1}' &\propto J_1(\beta_S)J_1(\beta_L)\{\cos[(\omega_S - \omega_L)t] \\ &\quad + \cos[(\omega_L - \omega_{IM})t]\} \\ i_{Q_1}' &\propto J_1(\beta_S)J_1(\beta_L)\{\sin[(\omega_S - \omega_L)t] \\ &\quad - \sin[(\omega_L - \omega_{IM})t]\}. \end{aligned} \tag{8}$$

Apply i_{I_1} and i_{Q_1} to a 90° electrical hybrid and the output signal is given by

$$\begin{aligned} i &= i_{I_1} + i_{Q_1}e^{j\frac{\pi}{2}} \\ &\propto J_1(\beta_S)J_1(\beta_L)\{\cos[(\omega_S - \omega_L)t] + \cos[(\omega_L \\ &\quad - \omega_{IM})t] + \cos[(\omega_S - \omega_L)t] - \cos[(\omega_L - \omega_{IM})t]\} \\ &= 2J_1(\beta_S)J_1(\beta_L)\cos[(\omega_S - \omega_L)t]. \end{aligned} \tag{9}$$

As can be seen from Eq. (9), The undesired component $\omega_L - \omega_{IM}$ is rejected. In this way, image rejection mixing is realized.

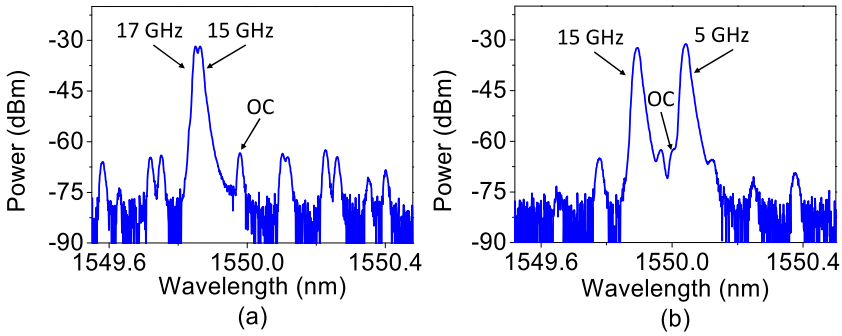

Fig. 2. Optical spectra of DP-DPMZM for (a) frequency down-conversion and (b) frequency up-conversion.

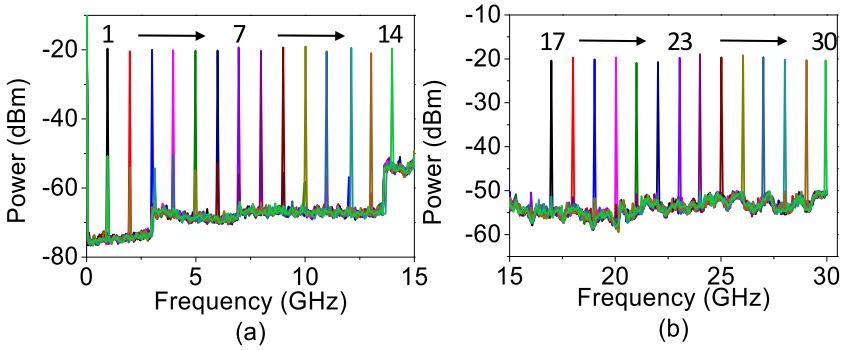

Fig. 3. Measured electrical spectra of the mixed electrical signal for (a) frequency down-conversion with RF signal tuned from 16 GHz to 29 GHz and (b) frequency up-conversion with IF signal tuned from 2 GHz to 15 GHz. The LO signal is 15 GHz.

3. Experiment

A proof-of-concept experiment was carried out to demonstrate the proposed reconfigurable MWP mixer. A 1550 nm OC was emitted from a LD and sent to a DP-DPMZM (Tektronix OM5110). A RF/IF signal and a LO signal were generated by a 40-GHz analog signal generator (Keysight N5183B) and a 20-GHz vector network analyzer and sent to the DP-DPMZM via two 90° electrical hybrids (Krytar 3017360K, 1.7–36 GHz), respectively. The bias voltage of the DP-DPMZM was set as described in the theoretical part to generate two orthogonally polarized CS-SSB signals. The generated orthogonal polarized CS-SSB signals were amplified by an EDFA (KEOPSYS CPO33). A PC and a PBS were used to separate the two CS-SSB signals which were then respectively sent to the signal and LO input port of the 90° optical hybrid (Kylia COH28). The PDs (Optilab LR40) used in the system have a bandwidth of 40 GHz. The electrical spectrum and waveform were measured by a 30-GHz spectrum analyzer (R&S FSP30) and a digital sampling oscilloscope (Tektronix DSA 8300), respectively.

Both DPMZMs of the DP-DPMZM worked as CS-SSB modulators, and the modulated optical signals for frequency down-conversion and up-conversion are shown in Fig. 2(a) and (b), respectively. As discussed in the theoretical part, the mixer can work either as a down-converter or an up-converter depending on the bias voltage φ_2 of the DP-DPMZM. Here, the LO signal was set at 15 GHz, and the RF signal for down-conversion was 17 GHz while the IF signal for up-conversion was 5 GHz. As can be seen, compared with the desired first-order sidebands, the OC and the unwanted sidebands are suppressed by more than 30 dB.

When one of the four output optical signals from the 90° optical hybrid was detected by a PD, a single-ended mixer can be realized. To demonstrate the wide tuning range of the single-ended mixer, we tuned the RF signal for down-conversion from 16 GHz to 29 GHz and the IF signal for up-conversion from 2 GHz to 15 GHz. With a fixed 15 GHz LO signal, a down-conversion range of 1–14 GHz and an up-conversion range of 17–30 GHz is respectively achieved, as shown in Fig. 3. It can be seen that the mixing spurs are suppressed by 30 dB. The tuning range of the mixer is limited by the bandwidth of the 90° electrical hybrids and the spectrum analyzer. It is worth noting that the noise floor in Fig. 3 increased sharply at 3 GHz and 14 GHz, which can be attributed to the uneven noise floor of the electrical spectrum analyzer.

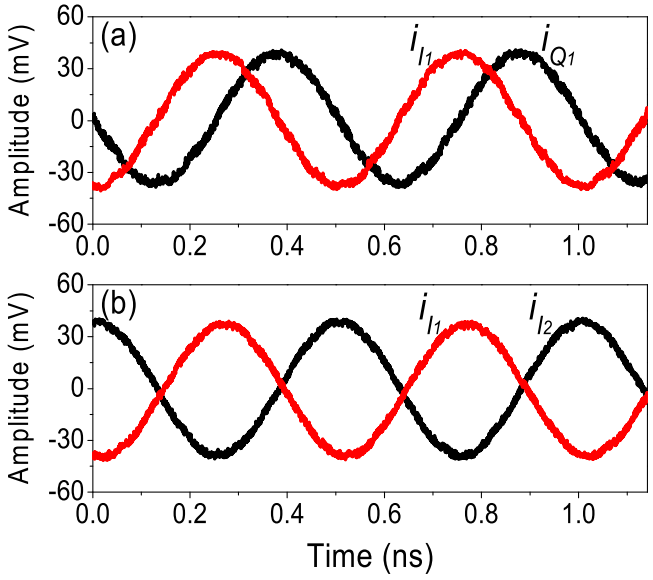

Fig. 4. Measured waveforms of (a) i_{I_1} and i_{Q_1} for the I/Q mixer and (b) i_{I_1} and i_{I_2} for the double-balanced mixer. Here, a 17 GHz signal is down-converted to 2 GHz.

The electrical output waveforms of the mixer with different detection configuration were measured and analyzed. First, the mixer worked as a down-converter, and a 17 GHz RF signal is down-converted to 2 GHz by

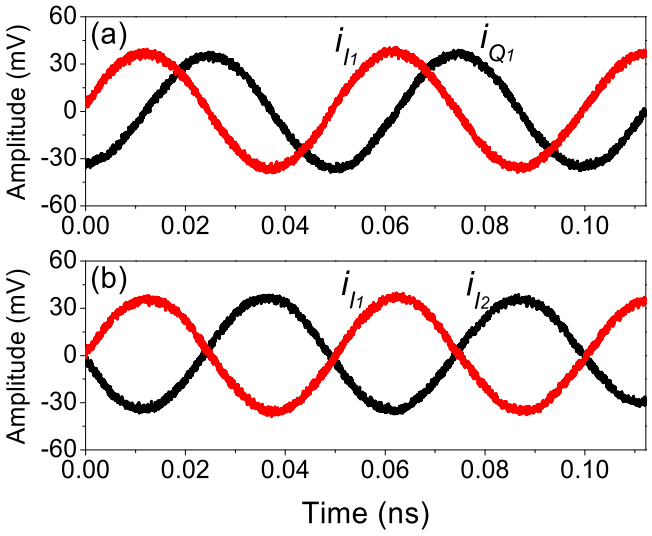

Fig. 5. Measured waveforms of (a) i_{I_1} and i_{Q_1} for the I/Q mixer and (b) i_{I_1} and i_{I_2} for the double-balanced mixer. Here, a 5 GHz signal is up-converted to 20 GHz.

a 15 GHz LO signal. Fig. 4(a) shows the waveforms of i_{I_1} and i_{Q_1} when output port I_1 and Q_1 were connected to PDs, while Fig. 4(b) is the waveforms of i_{I_1} and i_{I_2} when output port I_1 and I_2 were connected. It can be seen that i_{I_1} and i_{Q_1} have the same amplitude and a phase difference of $\pi/2$, while i_{I_1} and i_{I_2} have the same amplitude but a phase difference of π. This indicates that an I/Q mixer and a balanced mixer are respectively realized for frequency down-conversion.

By adjusting φ_2, the mixer was switched to an up-converter, and a 5 GHz IF signal was up-converted to 20 GHz by the same 15 GHz LO signal. Similarly, when output port I_1 and Q_1 were connected to PDs, the measured waveforms of i_{I_1} and i_{Q_1} is shown in Fig. 5(a), and when output port I_1 and I_2 were connected, the waveforms of i_{I_1} and i_{I_2} are shown in Fig. 5(b). It is clear that i_{I_1} and i_{Q_1} have identical amplitude and a phase difference of $\pi/2$, and i_{I_1} and i_{I_2} are of the same amplitude and a phase difference of π. Therefore, an I/Q mixer and a balanced mixer are respectively realized for frequency up-conversion.

Based on the I/Q down-converter, we used a 90° electrical hybrid (Krytar 3017360K) to combine i_{I_1} and i_{Q_1}. Here, a 17 GHz RF signal was down-converted to 2 GHz. As shown in Fig. 6(a), a 2 GHz IF signal with a power of −18.5 dBm is generated. To demonstrate image rejection, we introduced a 13 GHz signal to the system for down-conversion, and a 2 GHz image signal was generated. Fig. 6 shows the waveforms and spectra of the IF signal and the image signal. It can be seen that the down-converted image signal is −50.8 dBm, which is 32.3 dB lower compared with the useful IF signal. This means an image rejection mixer with an image rejection ratio (IRR) of over 32 dB is realized. The IRR can be further improved by using optical tunable delay line and optical variable attenuator to compensate for the amplitude and phase imbalance between the quadrature outputs of the 90° optical hybrid.

To demonstrate the tunability of the image rejection mixer, we changed the frequency of the input signals to show the tunable range of the mixer. In Fig. 7(a), the RF signal is tuned from 16.7 GHz to 20 GHz while the LO signal is fixed at 15 GHz. In Fig. 7(b), the LO signal is changed from 3.7 GHz to 30 GHz, and the IF frequency is 2 GHz. Here, a 40 GHz vector network analyzer is used to supply the LO signal. It can be seen that the IRR is over 30 dB when RF/LO signal is within 1.7–30 GHz and mixed IF signal is within 1.7–5 GHz. The lower limit of 1.7 GHz is restricted by the electrical hybrids while the upper limit of 5 GHz is mainly restricted by the imperfect frequency response of the DP-DPMZM. The upper limit can be further extended by employing optical tunable delay line and optical variable attenuator, as discussed in [23].

The performance of the proposed mixer is further analyzed with respect to the spurs free dynamic range (SFDR), the gain and the noise figure. To measure the SFDR of the system, a two-tone RF signal of 17 and 17.1 GHz was applied to the down-converter and a two-tone IF signal of 5 and 5.1 GHz was applied to the up-converter. As shown in Fig. 8, the SFDR of the frequency down-converter and the up-converter is 117 dB $Hz^{2/3}$ and 114 dB $Hz^{2/3}$ respectively for an assumed noise floor of −160 dBm/Hz. In addition, the noise figure and the gain of the system is measured to be 25 dB and −19 dB, respectively.

Compared with previous mixers, the proposed mixer have the following advantages: (1) instead of single-ended mixing reported in [12–15], this work achieves reconfigurable functions including single-ended mixing, double balanced mixing, I/Q mixing and image rejection mixing; (2) compared with [21,22], the proposed filter-free mixer enables a wide operating bandwidth and up/down-conversion function; (3) compared with [14,20,24], large SFDR is realized in this work since the 2nd order sideband is suppressed by the DP-DPMZM.

4. Conclusion

We have proposed and experimentally demonstrated a reconfigurable microwave photonic mixer based on DP-DPMZM. With different detection configurations, the mixer can perform single-ended mixing, double balanced mixing, I/Q mixing and image rejection mixing. Since no optical or electrical filter is used in the system, the operating bandwidth is improved. Furthermore, the mixer can switch between up-converter and down-converter. Experimental results show that the mixer has an operating bandwidth of 2–30 GHz and a spur suppression ratio of 30 dB. For image rejection mixing, the IRR is over 30 dB. Due to the flexibility and wide operating bandwidth of the proposed reconfigurable mixer, it can find applications in radar and broadband wireless communication systems.

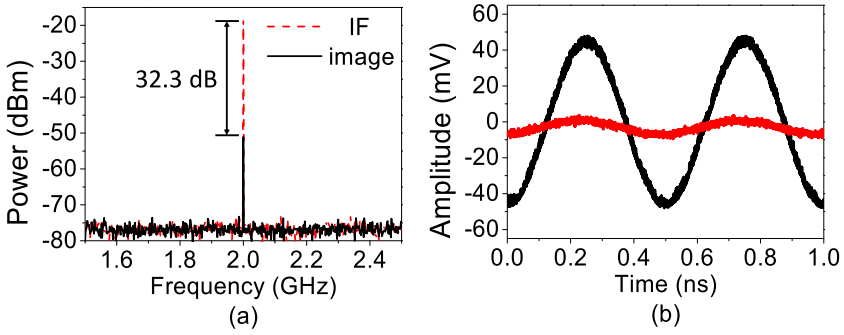

Fig. 6. Measured (a) spectra and (b) waveforms of IF and image signals after frequency down-conversion from the image rejection mixer.

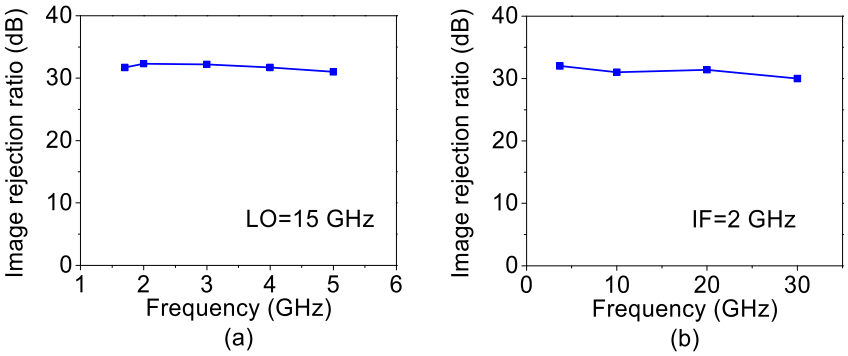

Fig. 7. Measured image rejection ratio with (a) RF tuned from 16.7–20 GHz and LO fixed at 15 GHz and (b) LO tuned from 3.7–30 GHz and IF at 2 GHz.

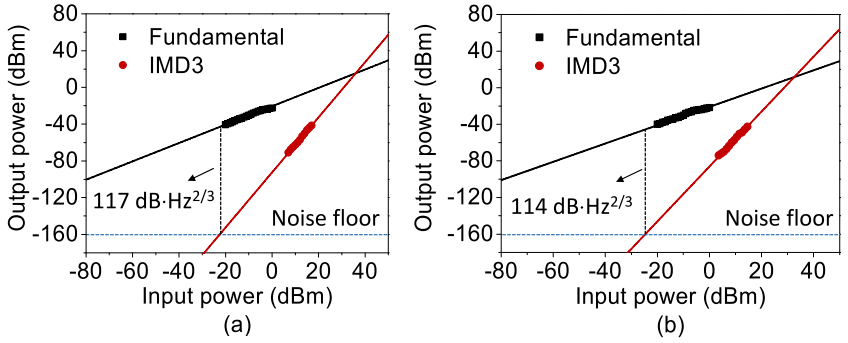

Fig. 8. Dynamic range performance of (a) the down-converter and (b) the up-converter. IMD3: third-order intermodulation distortion.

Acknowledgments

This work was supported in part by the National Natural Science Foundation of China under Grants 61335005, 61431003, 61335004, 61377069, and 61527820, in part by National High Technology Research and Development Program (863 Program) under Grant @015AA017002, and in part by Instrument Developing Project of the Chinese Academy of Sciences under Grant YZ201602.

References

[1] C.K. Sun, R.J. Orazi, S.A. Pappert, W.K. Burns, A photonic-link millimeter-wave mixer using cascaded optical modulators and harmonic carrier generation, IEEE Photonics Technol. Lett. 8 (1996) 1166–1168.
[2] A. Altaqui, E.H.W. Chan, R.A. Minasian, Microwave photonic mixer with high spurious-free dynamic range, Appl. Opt. 53 (2014) 3687–3695.
[3] S. Pan, D. Zhu, S. Liu, K. Xu, Y. Dai, T. Wang, J. Liu, N. Zhu, Y. Xue, N. Liu, Satellite payloads pay off, IEEE Microwave Mag. 16 (2015) 61–73.
[4] B. Benazet, M. Sotom, M. Maignan, J. Perdigues, Microwave photonics cross-connect repeater for telecommunication satellites, in: SPIE Photonics Europe, SPIE2006, p. 7.
[5] G.K. Gopalakrishnan, W.K. Burns, C.H. Bulmer, Microwave-optical mixing in LiNbO3 modulators, IEEE Trans. Microw. Theory Tech. 41 (1993) 2383–2391.
[6] R. Helkey, J.C. Twichell, C. Cox, A down-conversion optical link with RF gain, J. Lightwave Technol. 15 (1997) 956–961.
[7] M.M. Howerton, R.P. Moeller, G.K. Gopalakrishnan, W.K. Burns, Low-biased fiber-optic link for microwave downconversion, IEEE Photonics Technol. Lett. 8 (1996) 1692–1694.
[8] J.T. Gallo, K.D. Breuer, J.B. Wood, Millimeter-wave frequency converting fiber optic link modeling and results, in: Optical Science, Engineering and Instrumentation '97, SPIE1997, p. 8.
[9] Z. Tang, F. Zhang, S. Pan, Photonic microwave downconverter based on an optoelectronic oscillator using a single dual-drive Mach–Zehnder modulator, Opt. Express 22 (2014) 305–310.
[10] Q. Zhou, M.P. Fok, Microwave photonic mixer based on polarization rotation and polarization-dependent modulation, IEEE Photonics Technol. Lett. 27 (2015) 2453–2456.
[11] T. Jiang, S. Yu, R. Wu, D. Wang, W. Gu, Photonic downconversion with tunable wideband phase shift, Opt. Lett. 41 (2016) 2640–2643.
[12] E.H.W. Chan, R.A. Minasian, High conversion efficiency microwave photonic mixer based on stimulated Brillouin scattering carrier suppression technique, Opt. Lett. 38 (2013) 5292–5295.
[13] S.R.O. Connor, M.C. Gross, M.L. Dennis, T.R. Clark, Experimental demonstration of RF photonic downconversion from 4-40 GHz, in: 2009 International Topical Meeting on Microwave Photonics, 2009, pp. 1-3.
[14] E.H.W. Chan, R.A. Minasian, Microwave photonic downconverter with high conversion efficiency, J. Lightwave Technol. 30 (2012) 3580–3585.
[15] C. Bohemond, T. Rampone, A. Sharaiha, Performances of a photonic microwave mixer based on cross-gain modulation in a semiconductor optical amplifier, J. Lightwave Technol. 29 (2011) 2402–2409.
[16] T.R. Clark, S.R.O. Connor, M.L. Dennis, A Phase-modulation I/Q-demodulation microwave-to-digital photonic link, IEEE Trans. Microw. Theory Tech. 58 (2010) 3039–3058.
[17] Y. Gao, A. Wen, W. Jiang, Y. Fan, D. Zhou, Y. He, Wideband photonic microwave SSB up-converter and I/Q modulator, J. Lightwave Technol. 35 (2017) 4023–4032.
[18] S.A. Maas, Microwave Mixers, Artech House, Norwood, MA, 1986.
[19] C. Lu, W. Chen, J.F. Shiang, Photonic mixers and image-rejection mixers for optical scm systems, IEEE Trans. Microw. Theory Tech. 45 (1997) 1478–1480.
[20] S.J. Strutz, K.J. Williams, A 0.8-8.8-GHz image rejection microwave photonic downconverter, IEEE Photonics Technol. Lett. 12 (2000) 1376–1378.
[21] Z. Tang, S. Pan, A reconfigurable photonic microwave mixer using a 90 deg. Optical hybrid, IEEE Trans. Microw. Theory Tech. 64 (2016) 3017–3025.
[22] Z. Tang, S. Pan, Reconfigurable microwave photonic mixer with minimized path separation and large suppression of mixing spurs, Opt. Lett. 42 (2017) 33–36.
[23] J. Zhang, E.H.W. Chan, X. Wang, X. Feng, B. Guan, High conversion efficiency photonic microwave mixer with image rejection capability, IEEE Photonics J. 8 (2016) 1–11.
[24] V.R. Pagán, B.M. Haas, T.E. Murphy, Linearized electrooptic microwave downconversion using phase modulation and optical filtering, Opt. Express 19 (2011) 883–895.